Progress In Electromagnetics Research C, Vol. 135, 23–34, 2023

A 3 dB Compact UWB Hybrid Coupler for 5G Millimeter-Wave Applications

Mohamed Atef Abbas[1, 2], Abdelmegeed M. Allam[3], Abdelhamid Gaafar[2], Hadia M. S. El-Hennawy[1], and Mohamed Fathy Abo Sree[2, *]

Abstract—This paper presents a 3 dB compact Ultra-Wide-Band (UWB) Substrate Integrated Gap Waveguide (SIGW) based hybrid coupler suitable for 5G mm-wave applications. It is a key component in signal processing for wireless communication. It provides a way to control the power distribution of the signal along different ports. It could be used to achieve beamforming and adaptive antenna system. The design steps started with implementing a unit cell of the gap waveguide structure satisfying the required bandwidth of the coupler. A supercell is then implemented. A network of complete ridges is constructed. A further step is to design a coupling section which achieves the required power distribution along the coupling and isolated ports. This coupling section is implemented using a novel approach of inserting an elliptical slot with variable major and minor axes with a certain orientation that achieves the standard performance of a 3 dB directional coupler with $90^\circ \pm 5\%$ phase shift. For precise adjustment of this amplitude and phase, vias are further added perpendicular to the major axis of the slot. Its dimension and location have to be optimized. The Finite-Integral-Time-Domain (FDTD) analysis method is adopted (CST Microwave Studio). In addition, another novel approach is developed on this coupler such that the transition and gap layer is implemented on the same PCB layer, which saves the number of layers to only two layers compared to the usual three layers used in literature. Also, using SIGW technology saves the collapse of the top ground layer on the ridge structure, and only plastic pins are used to fix the two layers. The proposed coupler is fabricated and tested, and the results show that it serves the majority of frequency bands employed in 5G systems in the USA and Canada.

1. INTRODUCTION

The fifth generation (5G) of wireless communication technology has revolutionized how we use the internet and interact with the world around us, offering high-speed data for users, improved capacity, and reliability for their communication applications. The key to 5G technology is the use of millimeter wave (mm-wave) frequency bands, which provide the necessary bandwidth for 5G services. One of the most critical parts of this technology is the microwave and mm-wave components, which can bring tremendous boosts in data delivery speed and capacity. This cutting-edge technology has enabled us to reach a new level of performance, and transmit and access data more quickly and reliably than ever before. With these components, future generations will be able to take advantage of the latest technologies in a way that was impossible for previous generations [1–4].

Microwave components are a type of electronic circuit that is designed to work at frequencies in the microwave range, which are frequencies between 300 MHz and 300 GHz. On the other hand, millimeter wave components are designed to work at frequencies between 30 and 300 GHz [5]. Common

Received 27 April 2023, Accepted 14 June 2023, Scheduled 19 July 2023

* Corresponding author: Mohamed Fathy Abo Sree (mohamed.fathy@aast.edu).

[1] Department of Electronics and Communications Engineering, Ain Shams University, Cairo 11566, Egypt. [2] Department of Electronics and Communications Engineering, Arab Academy for Science, Technology and Maritime Transport, Cairo 11799, Egypt. [3] Information Technology, GUC, Cairo 101516, Egypt.

components used at these frequencies include antennas, couplers, filters, amplifiers, oscillators, and mixers. They are used in a variety of applications, such as 5G wireless communication, medical imaging applications, radar, satellite communication, Wi-Fi, and Bluetooth. The components used for millimeter wave applications are often more expensive than those used for microwave applications, as they require more advanced technology [6].

Directional couplers are really vital in the microwave and mm-wave range and are employed for a lot of different objectives. They can be utilized to sample the power of a wave, to transport power from one line to another, to merge signals, and to separate signals from each other. Directional couplers are also used in antenna systems to measure the power of the signal that has been acquired by the antenna. Directional couplers are of great importance for many reasons, such as their capacity to measure the strength of waves going through them. The amount of power that is coupled can range from a few milliwatts to several watts, depending on the design of the directional coupler. Directional couplers are typically used in radio transmitters and receivers to couple the output of the transmitter to the antenna or to couple the antenna to the receiver. They are also used in other RF systems, such as amplifiers, filters, and antennas. Directional couplers are typically designed to have a specific frequency response and impedance, which achieve the design process requirements [7, 8].

Many researchers have made significant progress in designing a hybrid coupler using different technologies, such as rectangular waveguides and microstrip (MS) lines [9, 10]. However, these structures present certain drawbacks, such as significant dispersion in rectangular waveguides and material and radiation loss in MS, which make them unsuitable for mm-wave frequencies. To address these issues, more efficient guiding structures such as a ridge gap waveguide (RGW) [11, 12], printed ridge gap waveguide (PRGW) [13, 14], and substrate-integrated gap waveguide (SIGW) have been proposed, offering improved performance with more compact, cost-effective designs and low-loss solutions suitable for high-frequency applications [15, 16]. RGW was introduced in 2009 by Kildal [17] through CNC machining but with an unstable gap height. Subsequently, in 2012, PRGW was suggested, providing a smaller footprint but still relying on an air gap. Finally, in 2016, the air gap was replaced by a dielectric substrate, creating the SIGW. This delivered more stability in the gap height with additional design freedoms that made it more engaging. As a result, those technologies have been used to design and implement various components across a wide range of frequencies, including microwave range and mm-wave range [18–23].

Through this paper, we present a 3 dB hybrid coupler operating at 30.5 GHz with a 10 GHz bandwidth, which offers extensive coverage of different frequency bands and is an ideal solution for 5G mm-wave applications. It also discusses a novel and unique technique for designing and fabricating this coupler, as well as a detailed step-by-step guide for researchers to implement this design easily or to use it when designing any microwave or mm-wave components based on SIGW. The paper is divided into four parts. Section 2 provides a comprehensive overview of the SIGW and coupler design, as well as the benefits of this proposed design. Section 3 offers experimental validation results and a discussion of the performance of the coupler. Lastly, Section 4 summarizes our results and makes recommendations for future work.

2. RGW AND SIGW TECHNOLOGY

RGW and SIGW are two faces of the same technologies that have revolutionized the world of microwave communication systems. The use of those technologies has enabled the development of high-performance and cost-effective microwave systems that are capable of transmitting signals over large distances. RGWs are a type of waveguide that utilizes a gap between two metal plates to guide the electromagnetic wave, while SIGWs utilize a dielectric substrate to guide the wave. Both have advantages and disadvantages, but SIGW has several advantages over RGW, where the air gap is substituted for a dielectric material. This guarantees a consistent gap height, thereby minimizing the risk of the gap collapsing due to stress. Additionally, the fabrication process is not complicated as RGW. The downside of the RGW with an air-filled construction necessitates extremely precise CNC machining, and its performance can be unpredictable. Inside the gap, a quasi-TEM state is maintained over the ridge, thus stopping electromagnetic (EM) leakage [23]. Consequently, our proposed design is based on SIGW technology. Therefore, the following subsection will discuss SIGW and its associated design procedures.

2.1. Theory of the Proposed SIGW Coupler

SIGW technology [13] is formed when two parallel conducting metallic plates — one a perfect magnetic conductor (PMC) and the other a perfect electric conductor (PEC) — are positioned with a dielectric material height less than $\lambda/4$. This configuration creates a stopband that stops parallel plate modes from propagating. In addition, metal ridges are strategically positioned on the PMC layer to direct the wave in one particular direction, while surrounding periodic structures of vias and blocks impede the wave from moving in the other direction. This technology offers numerous advantages, including a constant gap height and simpler fabrication. Inside the gap, the ridge sustains a quasi-TEM condition, and electromagnetic (EM) leakage is blocked.

2.2. Structure of the Proposed SIGW Coupler

Our current design employs the SIGW technology of two parallel layers. The bottom layer is called ridge layer. It is implemented using a Rogers RT5880 ($\epsilon r = 2.2$) substrate, with the ground and conductor mushroom patches linked by vias, which represents the periodic structure of the unit cell. It includes the directing ridge, which is situated between the upper and lower substrates. It produces the intended propagating way to the quasi-TEM mode. The top layer is called gap layer, which consists of the top ground and dielectric gap. It is implemented using a Rogers RO4003C ($\epsilon r = 3.55$) substrate. Figure 1 shows a structure of a sample unit cell of the SIGW constellation. The representation of the unit cell's dispersion diagram is represented in the same figure. One can notice that the band gap of the SIGW structure covers the frequency band from 20 GHz to 39 GHz. It is calculated by finite integrated time domain (FDTD) analysis using Eigen Mode Solver in (CST Microwave Studio). This band matches the required band of the proposed directional coupler in the mm-wave band. The dimension of this unit cell is determined according to the systematic process mentioned in [25] for the unit cell characterization. The supercell, including the ridge in the middle with width w, is illustrated in Figure 2. The depression diagram results in a frequency range of 21.6 GHz to 37.7 GHz. It is clear that the insertion of the ridge decreases the stopband by approximately 7%, as shown in Figure 2. The ridge width is optimized, and finding that the optimum width is 1 mm ensures effective transmission of the quasi-TEM mode signal over the whole band. The dimensions of the unit cell and supercell structure are provided in Table 1.

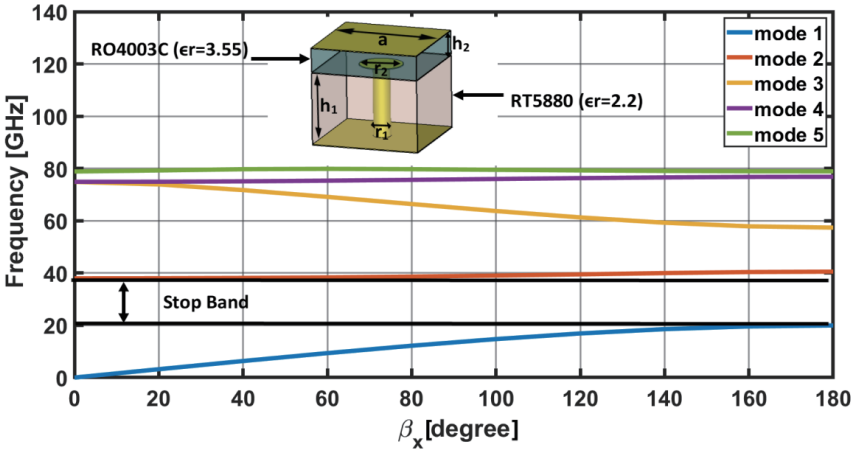

Figure 1. Structure of the sample unit cell and its dispersion diagram.

To confirm that the quasi-TEM mode propagates over the ridge, the electric field and current distribution are shown along the structure in Figure 3 and Figure 4, with the top layer hidden. Two frequencies are selected inside the band (28 GHz and 30.5 GHz), and the others are chosen outside the band (15 GHz and 40 GHz). The results of this analysis can be seen in Figure 3 and Figure 4. It is noticed that the E field and current distribution are confined within the ridge at 28 GHz and 30.5 GHz, and leakage occurs at 15 GHz and 40 GHz.

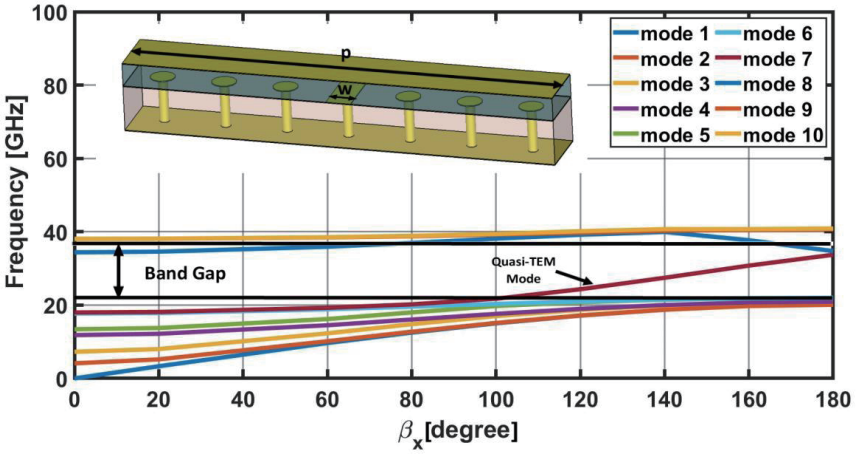

Figure 2. Structure of the sample supercell and its dispersion diagram.

Table 1. Dimensions of the two structures of the unit cell and supercell.

Symbol	Quantity	Value (in mm)
a	unit cell period	2.5
r_1	Diameter of Via	0.4
r_2	Diameter of the mushroom patch	1
h_1	The thickness of the base layer	0.508
h_2	The thickness of the ridge gap layer	0.203
w	Width of the ridge	1
p	Length of the supercell	17.5

For the design of the proposed novel directional coupler, the four ridges and coupling section are illustrated in Figure 5. Concerning the coupling section, it is composed of a rectangular patch of side length c with a 45° elliptical slot at the center. This side length is optimized in terms of a fraction of a quarter wavelength of the basic directional coupler. The elliptical slot major and minor axes are optimized to achieve the requirement of the coupling coefficient. It is found that the optimum values of c, d_1, and d_2 are 1.7 mm, 0.6 mm, and 2.8 mm. Additionally, the elliptical slot inclined angle is another control parameter which can control the power distribution in output ports. In this work, two additional vias are implemented orthogonal to the major axis of the slot for more precise adjustment of the output power, and the optimum value of b is 2.8 mm. All of these design parameters work together to create a symmetric and efficient connection and maximise the bandwidth while maintaining symmetry and ensuring equal power distribution in two output ports in addition to an isolated one.

A further design step is the implementation of a transition section from the microstrip line to the SIGW structure. It links the mm-wave signal from the SMA connector to the ridge to enable the measurements of the scattering parameters of the coupler. Figure 6 presents the microstrip line transition. It is implemented on Roger RO4003C, which is the same material used for the top gap layer of the SIGW structure. To achieve 50 Ω, the width of the microstrip line is 0.45 mm. For the sake of measurements of the mm-wave band, a special type of SMA connector with its mechanical adapter is mounted to the transition, as shown in Figure 7. This SIGW microstrip line transition is a reliable, cost-effective solution for microwave signal transmission. Finally, attaching an mm-wave edge SMA connector to the ridge is a hard task.

A further challenging step in the design is to match the microstrip line to the ridge. Through the usage of either the strip-line or the conventional microstrip line impedance equations, we can calculate the characteristic impedance of the ridge. Further optimization is carried out for the ridge with precise

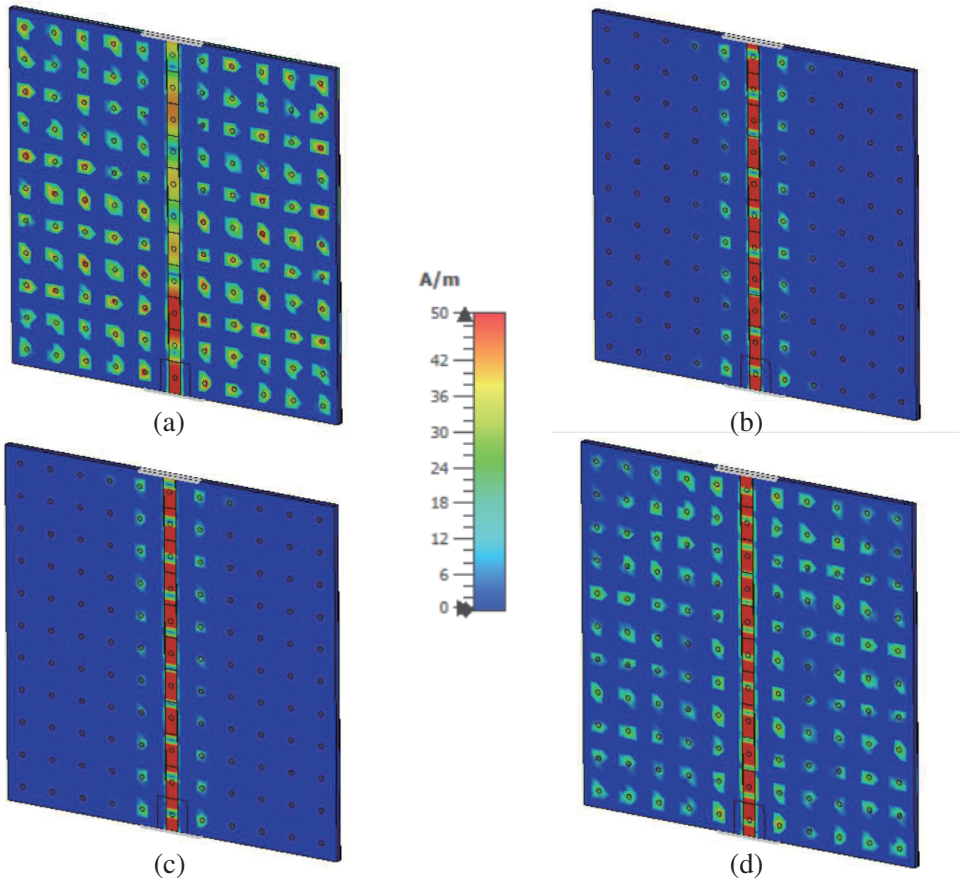

Figure 3. Surface current distribution at different frequencies. (a) 15 GHz (b) 28 GHz (c) 30.5 GHz (d) 40 GHz.

matching. Figure 8 shows the adjustment of the microstrip line over the ridge for power linking. This step is carried out for four ports. The optimum dimension is provided in Table 2.

Most of the similar published works in the literature implement three layers, two layers of the coupler (ridge layer and gap layer) and the transition layer. The novelty of the adopted work is the implementation of the transition layer with the top layer (gap layer) of the coupler on the same dielectric material using PCB technology, as shown in Figure 9.

Table 2. Dimensions of the SIGW microstrip line transition between ridge coupling section and SMA connector.

Symbol	Value (in mm)
f	0.45
t	0.8
w	1
l	2

2.3. Fabrication and Measurements Setup

Figure 10(a) represents the gap layer fabricated on roger RO4003C, while Figure 10(b) represents the ridge layer implemented on Roger RT5880. For the sake of measurements, the gap layer is connected

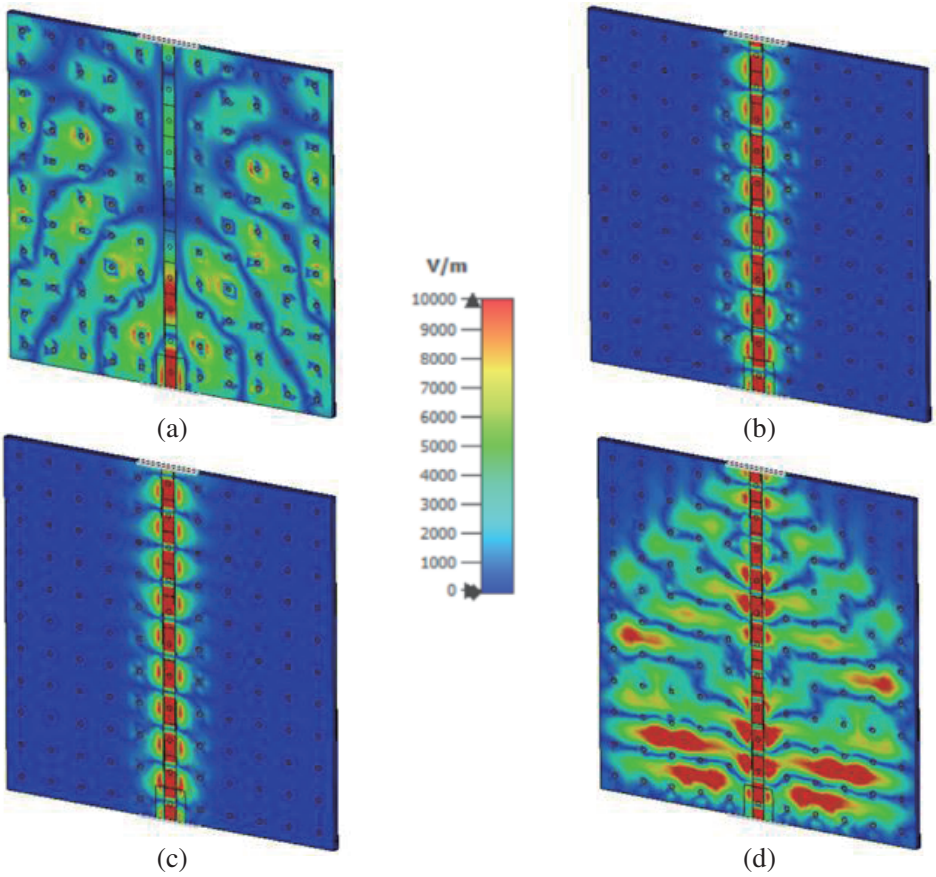

Figure 4. The E-field distribution at different frequencies. (a) 15 GHz (b) 28 GHz (c) 30.5 GHz (d) 40 GHz.

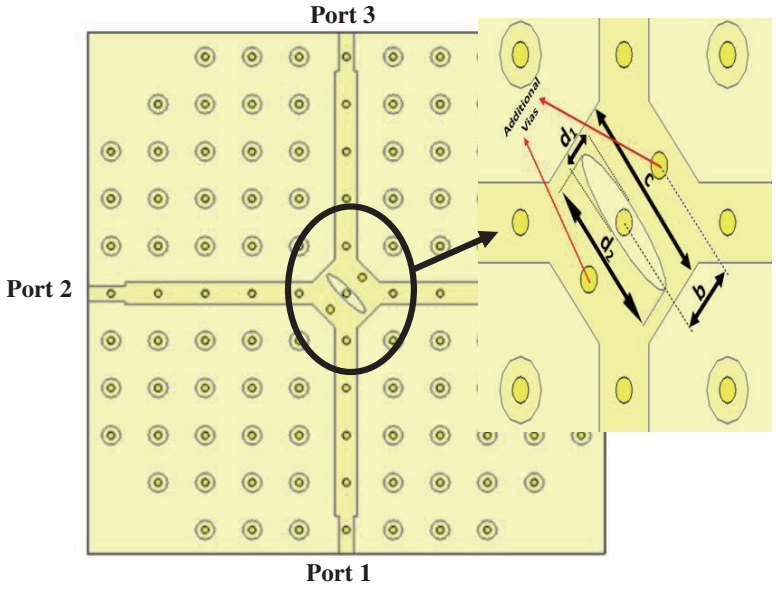

Figure 5. The proposed coupler structure.

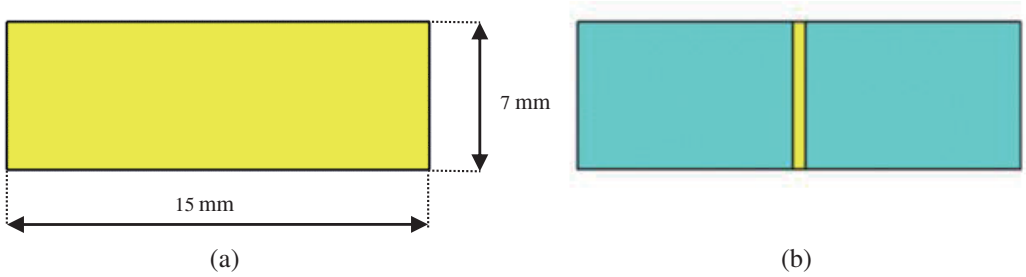

Figure 6. Microstrip line transition. (a) Top view. (b) Bottom view.

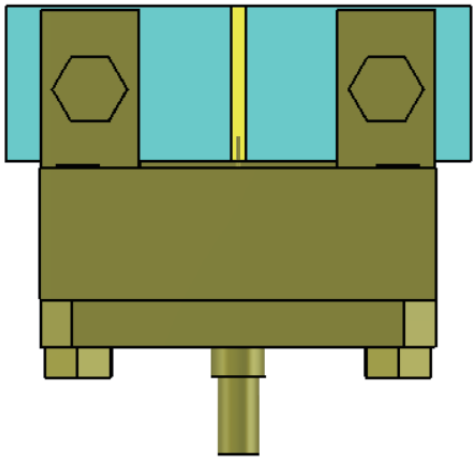

Figure 7. SMA connector mounting.

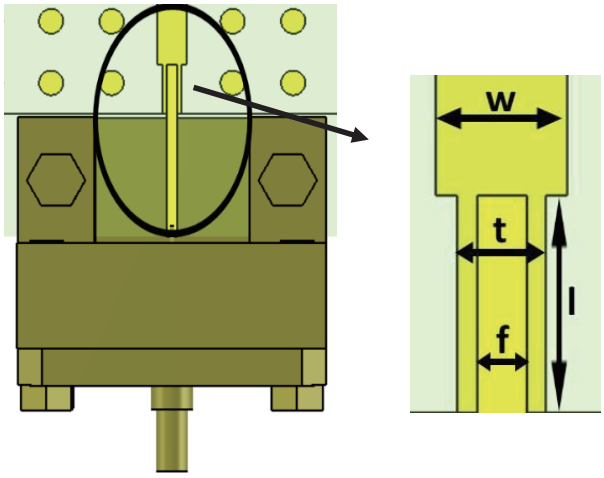

Figure 8. SIGW microstrip line transition with mm-wave connector.

to the mm-wave connector through a microstrip line transition, as depicted in Figure 10(c). To bind the gap and ridge layer together, plastic pins are used for fixation, as depicted in Figure 10(d), without distributing the performance of the coupler in the case of using metallic pins. The setup for scattering parameter measurements is shown in Figure 11 for different port configurations. ROHDE & SCHWARZ ZVA67 Vector Network Analyzer is used.

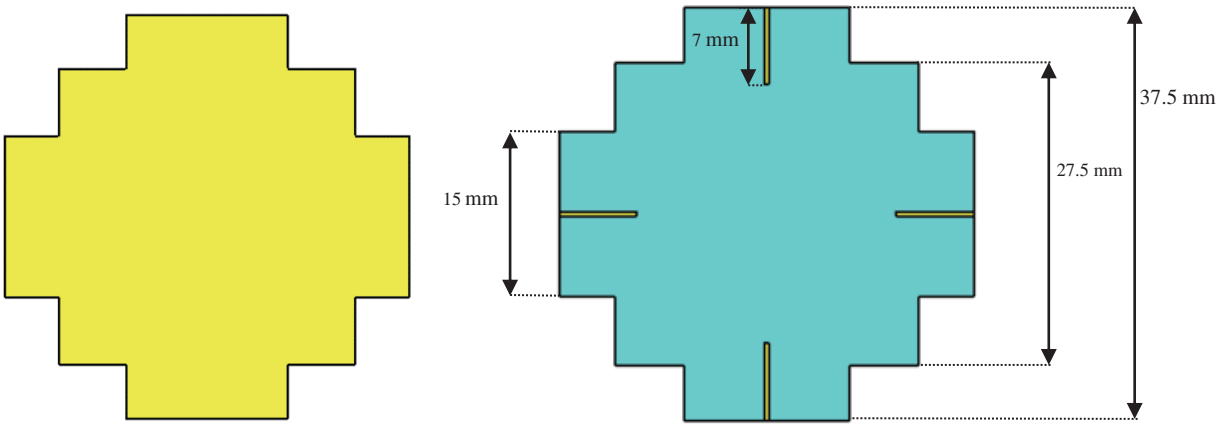

Figure 9. The gap layer of the proposed coupler with transition. (a) Top view. (b) Bottom view.

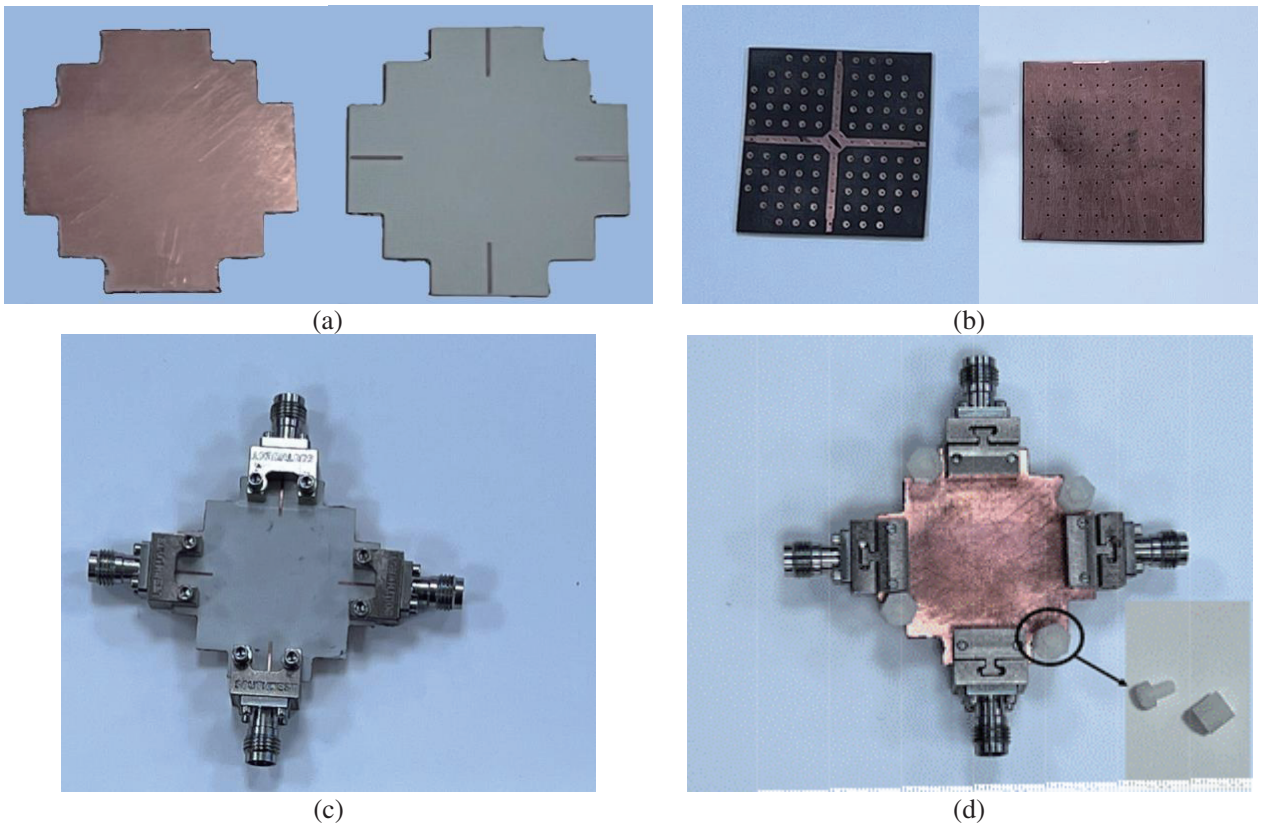

Figure 10. The fabricated coupler: (a) The Gap layer with transition (Top and Bottom views). (b) The Ridge layer (Top and Bottom views). (c) The Gap layer with the transition with mm-wave connectors. (d) The gap and ridge layers are bounded with fixation nails.

3. RESULTS AND DISCUSSION

Figure 12 shows the simulated and measured scattering parameters of the proposed coupler. It is evident that the design works between 27 and 37.5 GHz at a −10 dB level, and the coupling at the third and

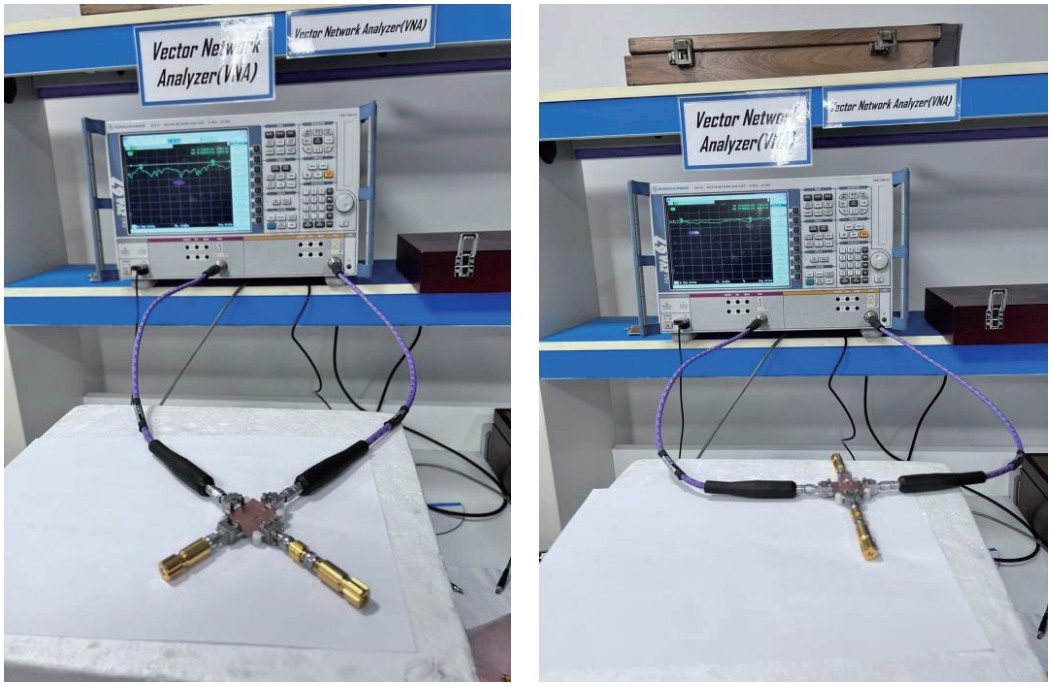

Figure 11. Measurement setup of the proposed coupler using ROHDE & SCHWARZ ZVA67 VNA [26] between different ports.

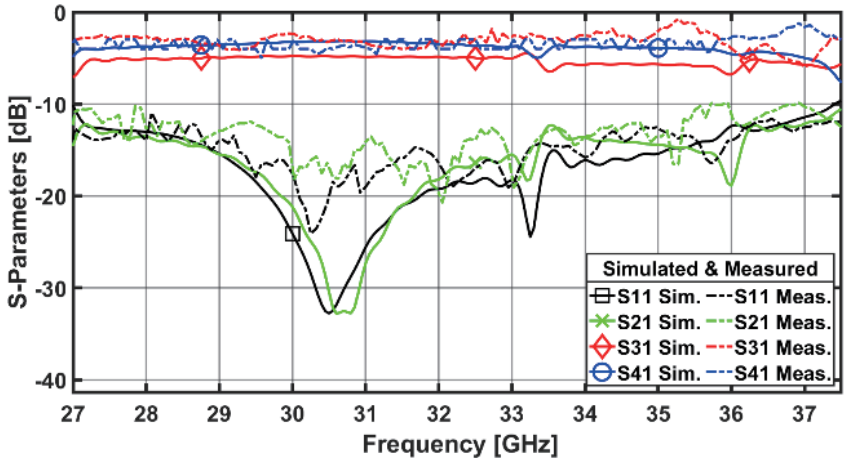

Figure 12. Simulated and measured S-parameters of the proposed coupler.

fourth ports is near 3 dB with an isolation of 30 dB at the second port. Figure 13 illustrates the phases of the output ports 3 and 4 and the phase difference between them. It is clear that the phase difference between them is $90° \pm 5\%$. It is also clear that the coupler achieves the hybrid parameters performance of basic 3 dB traditional couplers. A good agreement is found between the measured and simulated results, which verifies all the novel approaches of the SIGW coupler. The flow of the E field at 30.5 GHz is illustrated in Figure 14. It shows that the isolated port is changed according to the orientation of the elliptical slot implemented in the center of the coupling section.

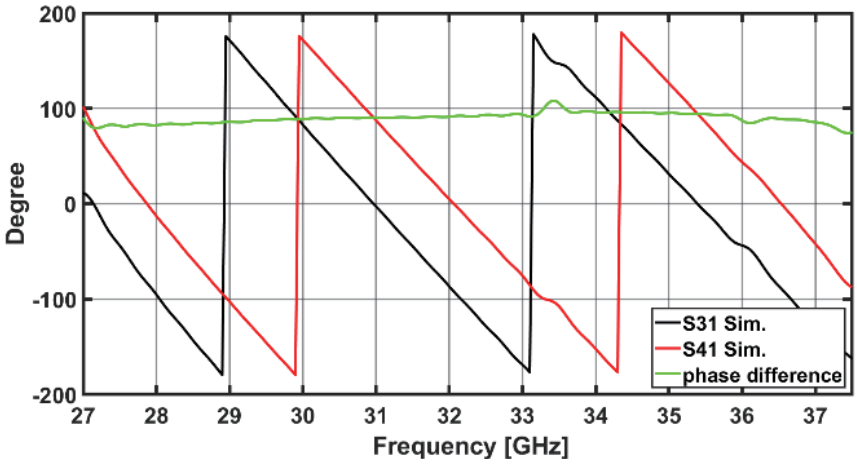

Figure 13. Phase responses in degrees between the third and fourth port.

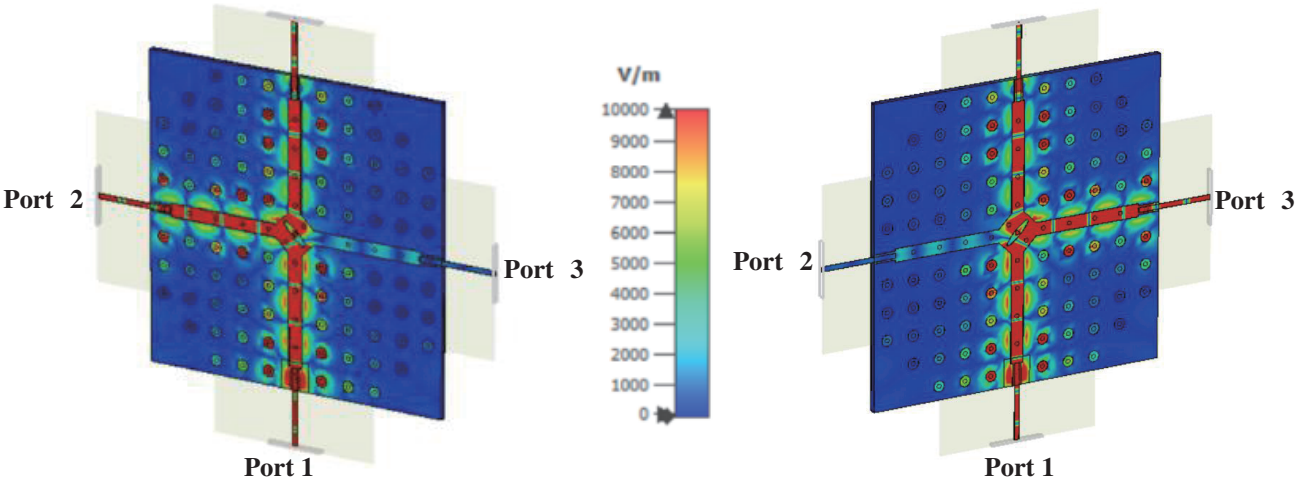

(a) (b)

Figure 14. The *E*-field distribution at 30.5 GHz. (a) Elliptical slot and additional vias are left inclined, (b) elliptical slot and additional vias are right inclined.

4. COMPARISON WITH PREVIOUS STUDIES

Table 3 shows a comparison between the proposed coupler and the most recent coupler works in the mm-wave frequency region. The analysis covers various coupler parameters, such as design technology,

Table 3. Comparison between the proposed coupler and previous studies.

Reference	[16]	[18]	[26]	Proposed
Technology	SIGW	PRGW	PRGW	SIGW
Freq. (GHz)	23.5–29	26–34	27.5–31.5	27–37.5
Fractional B.W (GHz%)	20.9%	26.6%	13.5%	32.5%
Return Loss (dB)	< -20 dB	< -15 dB	< -15 dB	< -10 dB
Phase difference	$90° \pm 3\%$	$90° \pm 5\%$	$90° \pm 10\%$	$90° \pm 9\%$
Number of Layers	3 (Fig. 16)	3 (Fig. 8(a))	3 (Fig. 7)	2 (Fig. 10)

number of layers, and other relevant coupler characteristics. The results of the comparison indicate that the proposed coupler is more efficient and has better performance in terms of all the parameters. Furthermore, it has a significantly lower insertion loss, which ensures that it can be used effectively in the mm-wave range. Additionally, It also has a much broader frequency bandwidth than the PRGW [19, 27] and even wider than the SIGW coupler [16]. Moreover, it employs a novel technique of implementing the transition in the same layer as the gap top layer of the coupler. This makes its manufacturability more convenient and cost-effective than the others.

5. CONCLUSION

The proposed novel SIGW-based coupler is designed, fabricated, and measured. It achieves the standard performance of a conventional directional coupler. The output of the coupling ports is 3 dB with a phase shift of 90° between them, and the isolation is 30 dB in the fourth port. The SIGW-based coupler operates over a wide band and is very compact with low insertion loss. The adapted approach has the very good advantage of implementing one layer for both the transition and gap layer of the coupler using the same dielectric substrate, which minimizes the complication of the structure. Additionally, a novel feature of the coupler is the insertion of an elliptical slot in the center of the coupling section, which provides a degree of freedom for exchanging the isolated port. Furthermore, it can give the potential to make a simple beamforming network which replaces the Butler matrix, can give more output ports, and as a consequence, give more shaped radiation patterns, which is used for conventional beamforming. Of course, it reduces the number of couplers and phase shifters in conventional beamforming networks. This can be implemented using more than four ridges without additional couplers or phase shifters. Also, in the top layer of the SIGW coupler structure, one can replace the ground with a metasurface of circular shape; when being rotated, it gives different amplitudes and phases of the output ports, which can achieve an adaptive beamforming system. The salient feature of this design is the generalization of design to be suitable for different frequency bands in 5G or 6G. One only needs to select the suitable unit cell of the SIGW structure of the ridge layer.

REFERENCES

1. Rappaport, T. S., S. Sun, R. Mayzus, et al., "Millimeter wave mobile communications for 5G cellular: It will work!" *IEEE Access*, Vol. 1, 335–349, 2013, doi: 10.1109/ACCESS.2013.2260813.
2. Fatah, S. Y. A., E. K. Hamad, W. Swelam, A. M. M. A. Allam, and H. A. Mohamed, "Design of compact 4-port MIMO antenna based on Minkowski fractal shape DGS for 5G applications," *Progress In Electromagnetics Research C*, Vol. 113, 123–136, 2021.
3. Emara, H. M., S. K. El Dyasti, H. H. Ghouz, M. F. A. Sree, and S. Y. A. Fatah, "Compact high gain microstrip array antenna using DGS structure for 5G applications," *Progress In Electromagnetics Research C*, Vol. 130, 213–225, 2023.
4. Rappaport, T. S., Y. Xing, O. Kanhere, et al., "Wireless communications and applications above 100 GHz: Opportunities and challenges for 6G and beyond," *IEEE Access*, Vol. 7, 78729–78757, 2019, doi: 10.1109/ACCESS.2019.2921522.
5. Pi, Z. and F. Khan, "An introduction to millimeter-wave mobile broadband systems," *IEEE Communications Magazine*, Vol. 49, No. 6, 101–107, Jun. 2011, doi: 10.1109/MCOM.2011.5783993.
6. Wu, K., M. Bozzi, and N. J. G. Fonseca, "Substrate integrated transmission lines: Review and applications," *IEEE Journal of Microwaves*, Vol. 1, No. 1, 345–363, Jan. 2021, doi: 10.1109/JMW.2020.3034379.
7. Kumar, S., A. S. Dixit, R. R. Malekar, H. D. Raut, and L. K. Shevada, "Fifth generation antennas: A comprehensive review of design and performance enhancement techniques," *IEEE Access*, Vol. 8, 163568–163593, 2020, doi: 10.1109/ACCESS.2020.3020952.
8. Ali AbdElraheem, M., M. Mamdouh M. Ali, I. Afifi, and A. R. Sebak, "Ridge gap waveguide beamforming components and antennas for millimeter-wave applications," *Hybrid Planar — 3D Waveguiding Technologies*, Jan. 2023, doi: 10.5772/intechopen.105653.

9. Rambabu, K. and J. Bornemann, "Analysis and design of profiled multi aperture stripline-to-microstrip couplers," *IEE Proc.-Microw., Antennas Propag.*, Vol. 150, No. 6, 484–488, Dec. 2003.
10. Jaisson, D., "Multilayer microstrip directional coupler with discrete coupling," *IEEE Trans. Microw. Theory Techn.*, Vol. 48, No. 9, 1591–1595, Sep. 2000.
11. Kildal, P.-S., E. Alfonso, A. Valero-Nogueira, and E. Rajo-Iglesias, "Local metamaterial-based waveguides in gaps between parallel metal plates," *IEEE Antennas Wireless Propag. Lett.*, Vol. 8, No. 4, 84–87, Apr. 2009.
12. Pucci, E., E. Rajo-Iglesias, and P.-S. Kildal, "New microstrip gap waveguide on mushroom-type EBG for packaging of microwave components," *IEEE Microw. Wireless Compon. Lett.*, Vol. 22, No. 3, 129–131, Mar. 2012.
13. Mahmoud Ali, M. M., S. I. Shams, and A. Sebak, "Ultra-wideband printed ridge gap waveguide hybrid directional coupler for millimetre wave applications," *IET Microw. Antennas Propag.*, Vol. 13, 1181–1187, 2019, https://doi.org/10.1049/iet-map.2018.5511.
14. Ali, M. M. M. and A. Sebak, "Compact printed ridge gap waveguide crossover for future 5G wireless communication system," *IEEE Microw. Wireless Compon. Lett.*, Vol. 28, No. 7, 549–551, Jul. 2018.
15. Zhang, J., X. Zhang, and D. Shen, "Design of substrate integrated gap waveguide," *2016 IEEE MTT-S International Microwave Symposium (IMS)*, San Francisco, CA, 2016, 1–4, doi: 10.1109/MWSYM.2016.7540186.
16. Shen, D., K. Wang, and X. Zhang, "A substrate integrated gap waveguide based wideband 3-dB coupler for 5G applications," *IEEE Access*, Vol. 6, 66798–66806, 2018, doi: 10.1109/ACCESS.2018.2879438.
17. Kildal, P.-S., "Waveguides and transmission lines in gaps between parallel conducting surfaces," Patent US20110181373A1, 2009.
18. Shams, S. I. and A. A. Kishk, "Design of 3-dB hybrid coupler based on RGW technology," *IEEE Transactions on Microwave Theory and Techniques*, Vol. 65, No. 10, 3849–3855, Oct. 2017, doi: 10.1109/TMTT.2017.2690298.
19. Ali, M. M. M., M. S. El-Gendy, M. Al-Hasan, I. B. Mabrouk, A. Sebak, and T. A. Denidni, "A systematic design of a compact wideband hybrid directional coupler based on printed RGW technology," *IEEE Access*, Vol. 9, 56765–56772, 2021.
20. Ali, M. M. M., S. I. Shams, and A. R. Sebak, "Printed ridge gap waveguide 3-dB coupler: Analysis and design procedure," *IEEE Access*, Vol. 6, 8501–8509, 2018.
21. Nasr, M. A. and A. A. Kishk, "Analysis and design of broadband ridge-gap waveguide tight and loose hybrid couplers," *IEEE Trans. Microw. Theory Techn.*, Vol. 68, No. 8, 3368–3378, Aug. 2020.
22. Afifi, I. and A. R. Sebak, "Wideband printed ridge gap rat-race coupler for differential feeding antenna," *IEEE Access*, Vol. 8, 78228–78235, 2020.
23. Abbas, M. A., M. F. Cengiz, A. M. M. A. Allam, D. E. Fawzy, H. M. Elhennawy, and M. F. A. Sree, "A novel circular reconfigurable metasurface-based compact UWB hybrid coupler for Ku-band applications," *IEEE Access*, Vol. 10, 129781–129790, 2022, doi: 10.1109/ACCESS.2022.3228110.
24. Sharifi Sorkherizi, M. and A. A. Kishk, "Transition from microstrip to printed ridge gap waveguide for millimeter-wave application," *2015 IEEE International Symposium on Antennas and Propagation & USNC/URSI National Radio Science Meeting*, 1588–1589, Vancouver, BC, Canada, 2015, doi: 10.1109/APS.2015.7305183.
25. El-Din, M. S. H. S., H. El-Hennawy, A. M. M. A. Allam, et al., "Approach for determination of the stop band for ridge gap waveguide," *2020 7th International Conference on Electrical and Electronics Engineering (ICEEE)*, 72–75, Antalya, Turkey, 2020, doi: 10.1109/ICEEE49618.2020.9102494.
26. https://scdn.rohde-schwarz.com/ur/pws/dl_downloads/dl_common_library/dl_brochures_and_data-sheets/pdf_1/ZVA_dat-sw_en_5213-5680-22_v1400.pdf. (Accessed on 20 12 2021).
27. Zhao, Z. and T. A. Denidni, "Millimeter-wave printed-RGW hybrid coupler with symmetrical square feed," *IEEE Microw. Wireless Compon. Lett.*, Vol. 30, No. 2, 156–159, Feb. 2020.